Calorimetric study of localized helium films in disordering substrates

Charles J. Yeager, Lindsay M. Steele,* and Daniele Finotello
Department of Physics, Kent State University, Kent, Ohio 44242
(Received 23 November 1993)

Helium films of thickness less than the critical coverage for superfluid onset at $T=0$ K were studied using a high-resolution calorimetry technique. The films were adsorbed on three disordering substrates: a planar geometry as offered by Mylar tape, a cylindrical geometry as provided by Anopore membranes, and a randomly connected porous geometry as obtained from Millipore fibrous filter paper. The substrates were characterized by nitrogen adsorption isotherms and scanning electron microscropy. A heat-capacity "bump" centered at a temperature that decreases with increasing thickness is found in all cases. The presence of the bump is interpreted as a universal feature for localized helium films adsorbed in substrates introducing disorder. The parameters characterizing such a bump are nonuniversal. The heat-capacity results are analyzed using models for adsorption on heterogeneous substrates.

I. INTRODUCTION

Independent of the substrate onto which a film is adsorbed, a common or "universal" behavior is revealed: superfluidity is manifest only after the thickness d (or equivalently, coverage n) exceeds a substrate dependent critical value d_c (n_c). This is a direct consequence of the strong Van der Waals attraction between helium atoms and the underlying substrate. For most substrates n_c corresponds to one to two atomic layers, or, to thicknesses ranging between 3 and 6 Å. In this thickness regime helium films are viewed as inert or localized. Superfluid films of total coverage n are then modeled in terms of an "inert" or "localized" layer of coverage n_c tightly bound to the substrate, and an overlayer of thickness $n-n_c$. There is no exchange of atoms between them due to the complete screening of the substrate potential by the inert layer that permits the ^{4}He atoms which are residing above it to be free of any external potential.

Through recent developments, studies of the properties of thin-film superfluidity and the crossover from localized to superfluid coverages have become the center of renewed attention. An important question that arises concerns the role of disorder since a large number of experimental studies of adsorbed helium films often employ strongly disordering substrates. Porous Vycor glass and Mylar polyester film are two examples of extensively used disordering substrates.

The onset of superfluidity at the finite critical coverage has been viewed as a realization of Boson condensation in a random potential.[1-5] The interplay between the effect of a disordering potential due to the substrate and the interaction and exchange among ^{4}He atoms in the adsorbed film leads to a zero-temperature continuous phase transition between the localized "Bose glass" and the superfluid phase. The transition is tuned by adjusting the chemical potential through a critical value,[2] experimentally corresponding to increase the surface coverage through n_c. In this approach, the critical coverage is nonzero because of disorder and the superfluid onset at zero temperature is viewed as a metal to insulator type of transition.

Several experiments have been devoted to specific heat studies of localized films in disordering substrates. The pioneering work in Vycor glass by Brewer and coworkers[6] which found a T^2 dependence for the specific heat of helium films of coverage less than the critical coverage over the temperature range between 0.6 and 4 K, was later extended to 0.1 K by Trait and Reppy.[7] This study showed that the specific heat temperature dependence changed character at a coverage dependent temperature T_b which decreased with increasing coverage. Below T_b, the heat capacity sharply decreased suggesting that some excitation is freezing out. An extrapolation showed that T_b might approach 0 K for the critical coverage for superfluid onset. More recently, higher resolution work reaching even lower temperatures has strengthened such interpretation.[8]

Calorimetry work was also performed for localized helium films adsorbed in Xerogel porous glass.[9] The porosity in Xerogel ($\sim$60%) is a factor of 2 larger than that in Vycor and with a pore size on the order of 100 Å. There, a distinct specific heat "bump" was found. The temperature of the middle of the bump shifted towards lower temperatures with increasing coverage. With increasing coverage and the film becoming superfluid, the bump disappeared.

In Vycor and Xerogel at constant temperature, the heat capacity of helium films in the localized layer increased with coverage.[7,10] However, once the film became superfluid at that temperature, the heat capacity sharply decreased with coverage towards the bulk value which would be presumably achieved if the film's thickness reached macroscopic dimensions. This heat-capacity decrease, also seen in studies of superfluid films in the cylindrical pores of Nuclepore membranes,[11] has been interpreted in terms of the stiffening of phonon modes as one moves away from onset conditions, in terms of increased order (lower entropy) associated with a thicker superfluid film, or due to the decrease of the available surface area as the pores begin to fill.[7,10-12]

Stimulated by these results, we have performed a sys-

tematic specific heat study for localized helium films as a function of geometry and disordering substrate. The substrates employed are the nearly cylindrical pores of the recently available Anopore membranes[13] and the interconnected pores of Millipore fibrous filter paper.[14] We also include results using planar Mylar polyester film.[15] These are heat-capacity measurements for helium films adsorbed in these three substrates. Independent of the geometry (substrate), a "universal" heat-capacity bump centered at a coverage dependent temperature is found. The data are analyzed in terms of models for helium films adsorption in heterogeneous substrates and are contrasted to that in porous glasses.

The paper is organized as follows. First, the confining substrates are characterized via nitrogen adsorption isotherms and scanning electron microscopy (SEM). Second, the calorimetry technique employed and the experimental cells' construction are detailed. We proceed with a presentation and analysis of the data and conclude by discussing the main results and suggest future work.

II. SUBSTRATES, EXPERIMENTAL TECHNIQUE, AND CELLS

Aside from the extensively studied Mylar, Millipore fibrous filter paper and the newly available Anopore membranes, are not as well known. Hence, we first describe work that was devoted to the characterization of these two materials. The section concludes by presenting the ac calorimetry technique and detailing the experimental cells construction.

A. Substrate characterization

1. Anopore membranes

Inorganic Anopore membranes are produced through the anodic oxidation of aluminum.[16] When aluminum is anodized in certain acid electrolytes, a porous oxide is developed. It exhibits a uniform array of cells, each of them containing a cylindrical pore. In such an electrochemical process, manufacturing conditions are controlled very precisely with the anodizing voltage determining the pore size and the pore density. A highly reproducible pore structure with a narrow pore size distribution is thus produced. Available as disks 25 or 47 mm in diameter, 45 or 60 μm thick, they possess nearly cylindrical pores of nominal 2000 Å diameter. Designed for critical filtration purposes, the membranes include a polypropylene ring that is heat glued to the outer edge of the membrane. For the larger size Anopore, the active membrane is 43 mm in diameter.

After cutting a membrane using a razor blade and shaping it into a disk 10 mm in diameter, SEM photographs at several magnifications were taken. The high density of pores present is evident from Fig. 1(a) which shows an SEM photograph of the top of an Anopore membrane. From an analysis of several photographs, the porosity was estimated at 39% while it was determined that the pore density is $\sim 1.3\times 10^9$ pores/cm^2. This is nearly a factor of 5 higher than in the similar pore size Nuclepore membranes.[17] The SEM photograph of a cross section of Anopore, Fig. 1(b), clearly demonstrates the parallelism among the pores.

To determine the available surface area, Anopore was also studied through nitrogen adsorption isotherms using a cell containing 20 membranes. The cell was later enlarged to contain 40 membranes and the isotherm repeated. Prior to the isotherms and by room-temperature helium expansion into the membranes, we again estimated their porosity and found it consistent with the SEM results. A slightly larger porosity was obtained when using

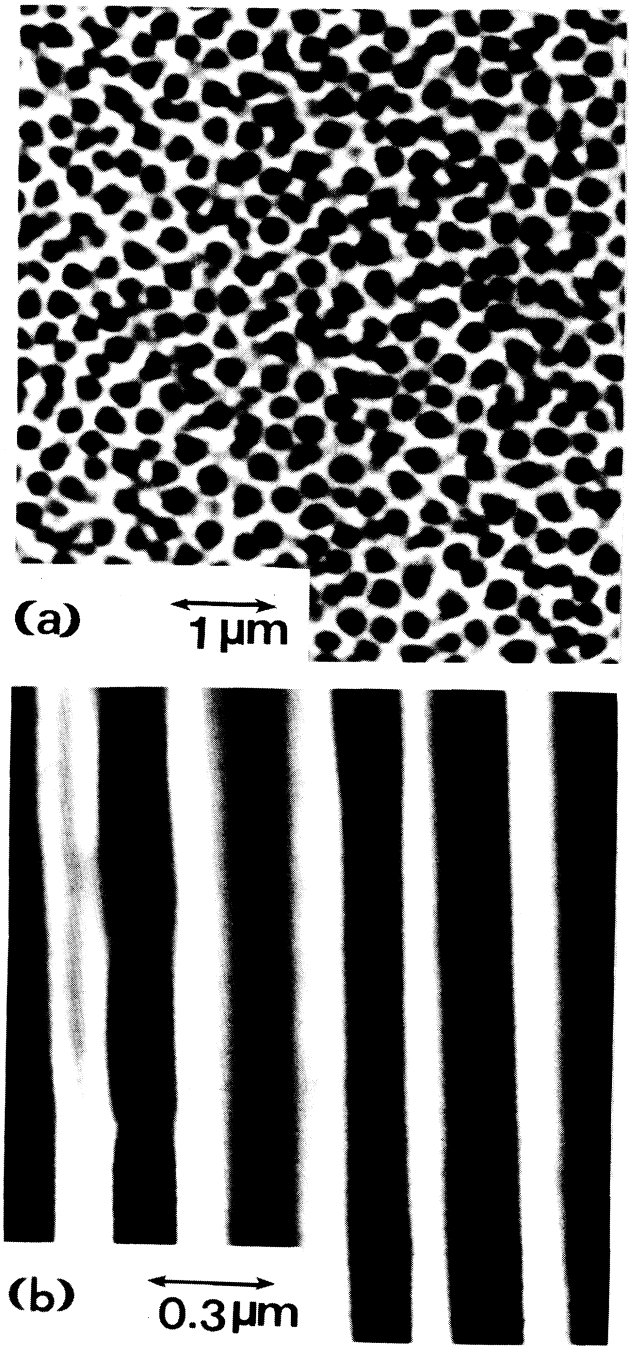

FIG. 1. Scanning electron microscopy photographs for an Anopore membrane. (a) top view (b) cross sectional view.

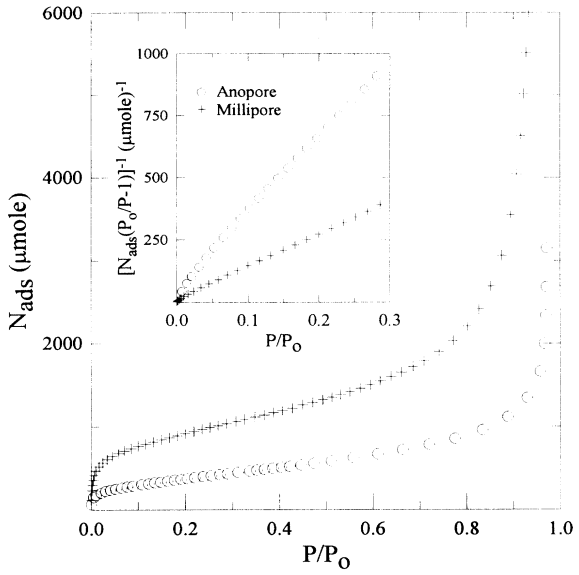

FIG. 2. Nitrogen-adsorption isotherms for Anopore and MIllipore. Each cell contained 40 membranes. Inset: BET plot to determine the surface area for both substrates. Solid lines represent fits to the data according to the BET equation.

FIG. 3. Scanning electron microscope photograph for a Millipore filter paper.

room-temperature nitrogen expansion. This was attributed to room-temperature nitrogen adsorption as also seen in Nuclepore.[17]

Figure 2 shows a 77 K isotherm for the cell containing 40 Anopore membranes, while the inset shows the standard Brunauer-Emmet-Teller (BET) analysis for multilayer adsorption in a heterogeneous media. The heterogeneity is evident from the rounded knee in the isotherm. From the BET analysis over the reduced pressure range between 0.05 and 0.3 in P/P_0 and using 16.2 Å^2 for the nitrogen adsorption cross sectional area, we determined the surface area to be 0.832 m^2/membrane which corresponds to 7.6 m^2/g given the 0.11 g mass of an Anopore membrane (excluding the plastic ring). This is twice as large than for Nuclepore, but considerably lower than for Vycor.[18] A complete discussion of the properties of Anopore in contrast to those of Nuclepore has appeared elsewhere.[19]

2. *Millipore fibrous filter paper*

Multiply connected Millipore fibrous filter paper is available in several disk diameters and different pore sizes. We used 115 μm thick, 47 mm diameter disks type VM with nominal 500 Å pore size. Surprisingly, but in agreement with previous observations,[20] upon inspection of an SEM photograph, Fig. 3, the characteristic pore size is actually a factor of ten larger. The diameter of the smallest fibers is on the order of 500 Å, while that of the largest fibers is near 2,000 Å.

Nitrogen adsorption isotherms were also performed for Millipore. A 77 K isotherm and the corresponding BET plot for the cell containing 40 Millipore filters, are also shown in Fig. 2. Since the mass of each filter is 0.098 g, we find a surface area of 20 m^2/g which is a factor of 3 larger than that in Anopore. From the adsorption isotherms, as P/P_0 approaches unity, the amount adsorbed in Anopore increases more sharply than in Millipore, a reflection of its narrower pore size distribution. For both substrates, 77 K isotherms were repeated using argon gas and the results for the surface areas reproduced to within 5%, the typical uncertainty associated with BET results.

3. *Mylar tape*

Mylar tape, a polyester film available from DuPont, has been extensively studied by a number of authors and in fact it has been the substrate of preference to probe two-dimensional properties of helium films. We refer the reader to the information available in the literature.[21]

B. Experimental technique and cells

ac calorimetry was used in these measurements.[22] The technique is quite suitable for low-temperature work since strict thermal isolation of the sample from the surroundings is not required. Computer control, averaging routines, and lock-in amplification techniques are easily implemented leading to high-resolution measurements.

In the ac technique, sinusoidal voltage heating at a frequency f is applied through a heater to the sample of interest. This induces temperature oscillations at a frequency $2f$ which are detected with a dc biased resistive thermometer; the amplitude of the induced oscillations is inversely related to the heat capacity of the sample. If the imposed oscillations are at a frequency "slower" than the sample internal equilibration time but "faster" than the external equilibration time (so that a negligible amount of heat is lost to the surrounding bath) as determined by repeated frequency scans at constant temperature,[23] the heat capacity of the sample can be calculated from

$$C = P_{PP}[32(\sqrt{2})\pi f T_{ac}]^{-1} , \quad (1)$$

where $P_{PP} = 4(V_p)^2/R$ is the peak-to-peak power dissi-

pated at the sample heater of resistance R, and T_{ac} are the induced temperature oscillations which are measured using a low-frequency lock-in amplifier operating in $2f$ mode. A schematic diagram of the heat-capacity data acquisition system is presented in Fig. 4(a).

The experimental cells were constructed as follows. Twenty Anopore were cut to a 2 cm diameter and tightly packed above one another inside a slightly larger diameter cuplike enclosure made from shim stock brass, 0.051 mm thick. The total mass of the membranes was 0.576 g, which given the nitrogen isotherms corresponds to a 4.37 m^2 surface area. The similarly constructed Millipore cell contained 10 filters of total mass 0.183 g and had a surface area of 3.66 m^2. Helium was admitted into the cells through a cupro-nickel capillary previously soldered to one face of the cell that also had an evanohm heater (0.0038 cm cross section, 28 Ω/cm) varnished to it. At the opposite face, a shaved 470 Ω speer resistor was varnished and served as the thermometer. The speer thermometers read about 800 Ω at room temperature and were calibrated at low temperatures against a calibrated germanium thermometer. A typical experimental cell is shown in Fig. 4(b).

For the Mylar cell we used a roll of tape 0.4 cm wide and 0.00076 cm thick. A 67.8 m length (mass 1.94 g) was formed into the so-called cylindrical jell-roll geometry[21] around the feed capillary. Brass shim was used to make two flat disks for the opposite faces of the cell which was sealed along its edges using a previously formed 1266 Stycast cylindrical housing. This cell was larger, 2.38 cm diameter, and three times thicker than either Anopore or Millipore. Its geometrical area is 0.54 m^2, which is used hereafter to label helium coverages. For Mylar,[21] it was found that the geometrical area was within 7% of the surface area determined by a 1.2 K isotherm.

For all cells, the operating frequency which ranged between 0.3 and 1.5 Hz, was independently determined by performing frequency scans at several temperatures for each film thickness. Every adsorbed film was annealed at least overnight at temperatures above 4.2 K. When required and due to a fast growing heat capacity with temperature, data were taken at different frequencies, heating voltages, and thermometer bias currents; the acquired data were overlapped considerably. Data were taken heating and cooling, and increasing and decreasing the film thickness.

III. RESULTS AND DISCUSSION

Given the planar nature of Mylar and the pore size in Anopore and Millipore being much larger than the film thickness (despite the pores' multiple connection in Millipore), helium films adsorbed in these substrates behave two dimensionally. Summarizing the major features of our results, the heat capacity at the lowest temperatures is difficult to resolve from the empty cells' contribution, yet, it is larger than bulk. No clear evidence of an underlying solidlike layer is found. For all substrates, a constant area specific heat bump centered at a temperature that decreases with increasing thickness is seen. This bump appears to be a universal feature for films adsorbed in disordering substrates. By renormalizing the specific heat and temperature scales by their values at the center of the bump, all data remarkably collapse onto a universal curve. Parameters typifying the bump, like its width and the lowest temperature at which it is seen, are substrate dependent, probably reflecting the competition or interplay between disorder and the Van der Waals attraction. The bump vanishes once the film is superfluid at the temperature where the bump would be expected.

A. Anopore

From the adsorption isotherm, the nitrogen monolayer completion per gram of Anopore membrane is 77.84 μmole. For the experimental cell used, this corresponds to 44.83 μmole of nitrogen. Based on the ratio of nitrogen to helium areal densities, the helium monolayer completion is estimated at 18.3 μmole/m^2. Alternatively, using a model where the first layer has the helium solid density and a thickness of 3.6 Å, the helium monolayer completion would be at 17.2 μmole/m^2, which is a factor of 1.676 larger than the measured nitrogen monolayer completion. An identical ratio was obtained from results of measurements of the helium and nitrogen monolayer completion in Nuclepore.[17] Subsequent layers are treated as liquid with a bulklike density of 0.145 g/cm^3 with one liquid layer corresponding to a coverage of 12.82

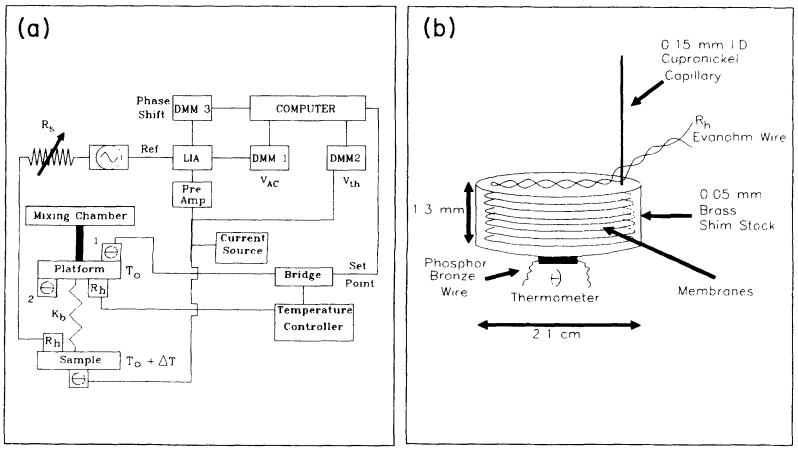

FIG. 4. (a) Schematics of the ac technique data acquisition system. θ_1 and θ_2 represent germanium thermometers while θ is the shaved speer. (b) Schematic of a typical ac heat-capacity cell.

μmole/m^2. As often employed with heterogeneous substrates, films are labeled in terms of coverage in μmole/m^2. The nature of these results is such that precise knowledge of the helium monolayer completion is not crucial.

Heat capacity results for the four thinnest (submonolayer) films studied in Anopore are shown in Fig. 5 where the empty cell contribution (not subtracted from the film's data) is indicated by the solid line. For these thicknesses and temperatures up to 2 K, the heat capacity is dominated by the addendum materials, in particular the brass shim, thermometer, and epoxy. The helium contribution is only about 1% above the background over the temperature range shown. The magnitude of the helium heat capacity changes (at most) from 0.3 erg/K at 0.3 K, to 3 erg/K at 2 K. Using the value of 0.3 erg/K at 0.3 K for the 12.25 μmole/m^2 coverage, its specific heat is 0.56 mJ/mole K, which is six times larger than that of bulk helium at the same temperature. This is not surprising because due to the underlying substrate and the available free surface, the excitation spectrum from films is expected to be richer than that of bulk. Given the large background attempting to extract the overall temperature dependence for these films would not be very reliable.

Strikingly, if the coverage is slightly increased, the helium contribution to the heat capacity becomes quite significant and deviates from the empty cell at progressively lower temperatures with increasing coverage. At temperatures below 0.4 K, the empty cell still remains the largest contribution to the total heat capacity. The specific heat for five films between 1 and 2 layers thick is shown in Fig. 6. The empty cell contribution, fitted to a polynomial in temperature, has been subtracted from these data. The emergence of a "bump" centered at a temperature that decreases with coverage is the major feature in these data. Interestingly, features whose position in temperature decreases with coverage have been found in porous glasses.[7–9]

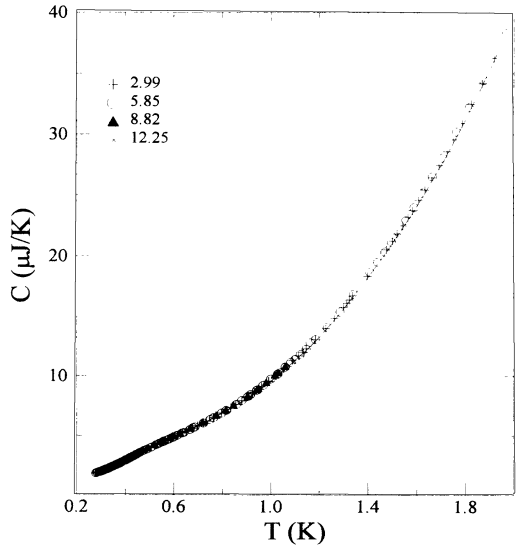

FIG. 5. Heat-capacity results for the four thinnest films studied in Anopore. Note that on the scale of the plot, the films' heat capacity lies on top of the empty cell contribution indicated by the solid line. Coverages are in μmole/m^2.

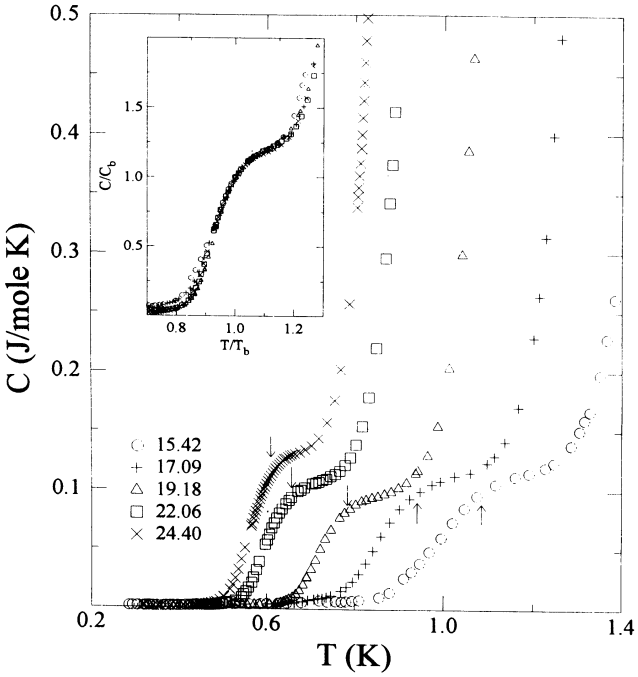

FIG. 6. Specific heat as a function of the temperature for five films in Anopore after empty cell subtraction. Coverages are in μmole/m^2. Note the bump shifting to low temperatures with increasing coverage. Arrows indicate the middle of the bump temperature (T_b). Inset: same data normalized by the specific heat and temperature at the middle of the bump to show the nearly perfect collapse of the data in a single universal curve.

The bump sharpens with coverage. Its temperature width decreases from 365 to 200 mK for the films shown. The specific heat magnitude at the middle of the bump above an arbitrarily chosen linear background increases by a factor of 1.8 in such a way that the area under the bump is nearly constant (to about 15%) of magnitude 4.2 mJ/mole suggesting that the underlying phenomena giving rise to the bump is independent of coverage. This is emphasized in the inset to Fig. 6, where the data for each film, normalized by the corresponding temperature (T_b) and specific heat (C_b) values at the middle of the bump, remarkably collapse onto a universal curve. If the coverage is further increased and the film is superfluid at the temperature where the bump would be expected, it disappears.[24] The presence of a bump appears to be a universal feature for localized films in disordering substrates. Bump parameters such as width, area, and temperature position, may be a measure of the interplay between substrate disorder and the Van der Waals attraction.

Studies of disorder effects have mostly dealt with superfluid properties and critical behavior, and have not included the ever present Van der Waals attraction to the substrate, thus, we have considered several possibilities to analyze these results. Due to surface roughness, helium atoms are localized in potential wells of linear dimensions equivalent to the surface roughness and whose depth

quantifies the Van der Waals attraction to the substrate.[25] The heat-capacity bump would then correspond to excitations from the ground to the first excited state. For a surface roughness on the order of 20 Å (which is, for instance, an upper surface roughness cutoff length in Vycor[18]) and a Van der Waals attraction of ~20 K, the energy difference between the ground and first excited state in such a potential well would be approximately 0.3 K, which is comparable to the width of the Anopore bumps. Once these low-lying excited states are filled, the bump disappears. The narrowing of the bump and its shifting to lower temperatures would be related to the screening of the substrate potential as the film thickens.

For Anopore, we do not have a reliable estimate for the surface roughness that would allow calculations for the size and depth of the potential well. Also, since a strikingly similar behavior is equally found in Millipore and Mylar, the surface roughness would have to be on the same length scale for all substrates. In addition, as briefly reported elsewhere,[26] a bump continuously shifting to much lower temperatures (~100 mK), and with a different coverage dependence was also found for ^{3}He films in Anopore. Interestingly, a shoulder appearing at a temperature that decreases with coverage has also been seen for the first and second layer of ^{3}He on ordered graphite.[27] Since the Van der Waals attraction does not distinguish between isotopes, the model would need to incorporate the larger zero-point motion and smaller mass of ^{3}He. Complementary studies, after preplating to smooth out the substrate and thus alter the Van der Waals attraction, would be informative. The complete ^{3}He work will be published separately.

Helium films on heterogeneous substrates have been discussed by Roy and Halsey[28] and Daunt.[29] As clearly detailed by Tait and Reppy,[7] it is argued that fluctuations in the adsorption potential are not randomly distributed across the surface. They are grouped together in such a way that they introduce long-range variations which in turn give rise to large lateral pressures on the adsorbed helium atoms. Although the substrate potential is not strong enough to localize the helium atoms at particular sites, the lateral pressures are strong enough to force helium atoms into patches or islands. The density of states is such that there is a gap in the excitation spectrum. The appropriate expressions for the heat capacity are[7]

$$C = A(\Delta/k_B T + 2)\exp(-\Delta/k_B T) + DT^2, \quad T < T_c, \ \Delta \gg k_B T , \tag{2}$$

and

$$C = B'T + D'T^2, \quad T > T_c, \ \Delta \ll k_B T , \tag{3}$$

where T_c is a cutoff temperature that decreases with coverage and Δ is the energy gap between the immobile adatom states and the free or extended (as suggested by Crowell[8] because of the nonnegligible He-He interaction) particle states. With increasing coverage, the islands merge and the gap disappears. For islands to form, the energy gap must be comparable to the Van der Waals constant.[8] The quadratic term describes the contribution from the adatom island which are assumed to behave like pseudo-Debye two-dimensional solids.

When Eqs. (2) and (3) were used to analyze the results for films in Vycor,[7] reasonable agreement was found with Δ/k_B ranging between 1 and 2 K. We also fitted the Xerogel data,[9] and found excellent agreement for $\Delta/k_B \sim 1$ K. The Anopore fits to Eq. (2), shown by solid lines in Fig. 7, find a Δ/k_B that decreases from 11.5 to 8.5 K with increasing coverage. Even though a Δ/k_B of 10 could reasonably fit all data, a slowly changing and decreasing Δ with coverage is expected due to the increased screening. The collapse of the data on the universal curve (inset to Fig. 6) is a result of the decrease in Δ simultaneously with the normalization of the temperature scale. The argument of the exponential function of Eq. (2) is unaffected by changes in the magnitude of the heat capacity. After the sharp rise and over a narrow temperature range, as seen from the plot of C/T against T of Fig. 7, the data are nearly horizontal indicating that the linear temperature dependence of Eq. (3) is dominant in this small-temperature regime.

A significant result is that Δ/k_B is five to six times larger than in porous glasses. A large Δ is needed for the islands to form.[8] In terms of the model where helium atoms are considered to be in potential wells of linear dimensions comparable to the surface roughness, this translates into a surface roughness on the order of 3.5 Å which is probably low and it cannot account for the bumps' temperature width. In the model described by Eqs. (2) and (3), where 2Δ is the magnitude of the variation of the potential energy of adsorption across the surface, strong deviations from the behavior predicted by Eq. (3) are seen at temperatures slightly above T_b. The magnitude of the gap energy Δ in Anopore, comparable

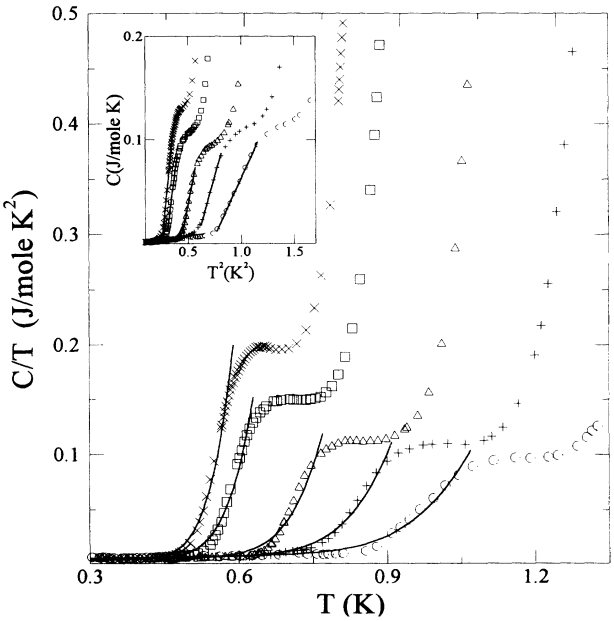

FIG. 7. Specific heat divided by temperature as a function of temperature. Symbols are as in Fig. 6. Fits to Eq. (2) are represented by the solid lines. Inset: same data plotted as a function of T^2. Solid lines, which have a negative intercept, are fits to the data.

to the attraction to the substrate and thus supportive of a picture of island formation, limits the applicability of Eq. (3) to much higher temperatures ($\Delta \ll k_B T$) than probed in these measurements. Also, with increasing coverage, the islands merge, superfluid behavior sets in, and the gap energy should disappear. However, given our estimate of $n_c \sim 20$ μmole/m^2, some of the films that show a heat-capacity bump are superfluid below the bump temperature. Thus, the bump is a property of the nonsuperfluid component of the film. An island formation picture does not appear to be the likely scenario in Anopore.

A similar view can be adopted in the understanding of the Vycor results. In Vycor, there exist higher-temperature data which extrapolates downwards with the temperature dependence predicted by Eq. (3) and smoothly merges with the low-temperature gaplike behavior near the break temperature, i.e., Eqs. (2) and (3) simultaneously fit the data over a wide temperature range. However, it is the small magnitude of Δ (~ 1 K) which may rule out the island formation picture to understand the Vycor results.

Concentrating only on the low-temperature data prior to the sharp rise, from Figs. 6 or 7, the heat-capacity data for all films can be described by a dominant linear temperature dependence in addition to a smaller quadratic one. A linear temperature dependence is typical and is expected for disordered systems[3] while the T^2 dependence would represent the contribution from an inert Debye-like layer. Unfortunately, given the large addendum we cannot distinguish whether these temperature dependencies are real or they are an artifact arising from the empty cell subtraction. Considering the existing theoretical interest, it would be important to design a cell that minimizes the addendum contribution (by an order of magnitude) thus allowing the possibility of unambiguously determining the presence of such terms.

If only specific heat data that unambiguously deviate from the background in its fast rise to the middle of the bump are considered, all films are well described by a quadratic temperature dependence as shown in the inset to Fig. 7. If the coefficients of this T^2 dependence are taken at face value, we determine Debye temperatures which decrease from 32 K for the 15.42 μmole/m^2 film to 15 K for the 24.39 μmole/m^2 film as a result of the additional screening in thicker films. These values are reasonable and consistent with those found in other substrates, yet, the heat capacity does not extrapolate to zero at $T=0$ K; in fact, there is a negative intercept. Hence, a T^2 dependence as expected for a two-dimensional (2D) solid layer does not provide a complete description of the data.

Any analysis of the heat-capacity temperature dependence in Anopore is further complicated by the existence of a subtle anomaly at higher temperature. This anomaly also shifts to lower temperatures with coverage. This is shown in Fig. 8 where the same helium films data of Fig. 6 are plotted over a wider temperature range. This anomaly has a nearly constant temperature width of 0.275 ± 0.02 K while the area increases from 12 to 30 mJ/mole with increasing coverage.

Due to the high temperatures, it is reasonable to suspect that it might arise from desorption whose contribution to the total heat capacity can be calculated from[30]

$$C = \{P_0 V/T;\}\{q_{ST}/k_B T\}^2 \exp(-q_{ST}/k_B T)\ , \qquad (4)$$

where P_0 is the saturated vapor pressure at 4.2 K and q_{ST} is the heat of adsorption defined as the amount of energy required to evaporate an atom from the film. V is the dead volume accessible to the vapor. From a plot of $\ln(CT^3)$ against T^{-1}, an activation energy plot, a straight line of slope equal to $-q_{ST}/k_B$ is expected. When our data are plotted in this fashion, as in the inset to Fig. 8, no well-defined linear region is found.

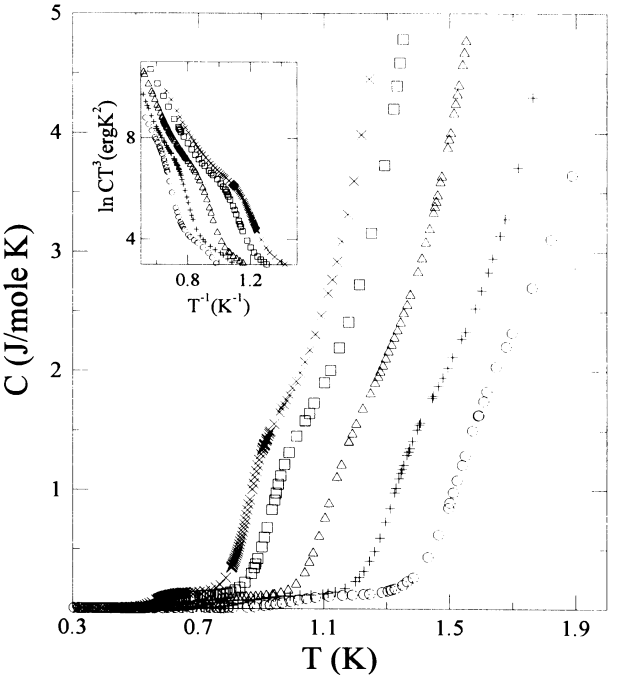

FIG. 8. Specific heat results for the Anopore films of Fig. 6, plotted over a wide temperature range. Note the appearance of a subtle anomaly of constant temperature width also shifting to low temperatures with coverage. Symbols as in Fig. 6. Inset: desorption contribution to the heat capacity. Data plotted according to Eq. (4).

We believe that this anomaly is present even for thicker and superfluid films that continuously shift to temperatures as low as 0.4 K films as thick as 60 μmole/m^2.[31] At some thickness, this anomaly appears to signal a region where a significant change in the heat-capacity temperature dependence is taking place as a result of changes in the film's excitation spectrum with thickness. As evident from Fig. 9, the anomaly temperature position (chosen at the middle after a linear background subtraction) exhibits a rather similar coverage dependence to that of the low-temperature bump, well characterized by $T_b \sim n^{-4/3}$, probably quantifying substrate effects. Thus, we do not believe that the high-temperature anomaly can be attributed to a desorption mechanism. We presently lack an explanation for this anomaly, measurements covering a finer grid of coverages after surface preplating would be important in determining its origin.

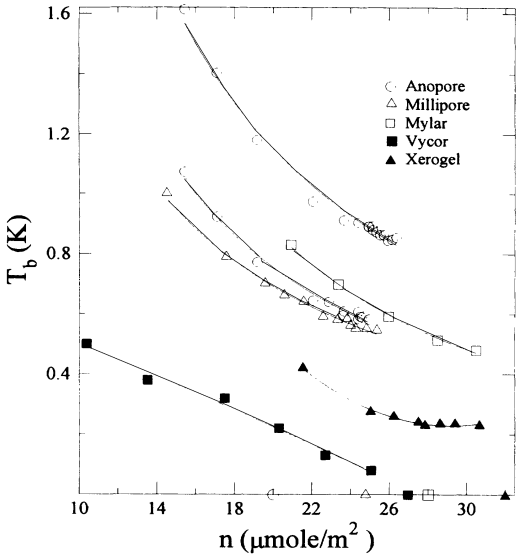

FIG. 9. Coverage dependence of the (middle) temperature position for Anopore (bump and high temperature anomaly), Millipore and Mylar. Also shown are the dependence for the bump position in Xerogel (Ref. 9) and the break in Vycor (Ref. 7). The Vycor results represent the temperature at which the heat-capacity temperature dependence changes drastically. Symbols on the horizontal axis corresponds to the critical coverage for each substrate. Lines are guides to the eye.

As an alternative, we have also attempted to view the low-temperature bump as an indication that some of the helium is undergoing some kind of transition. Hence, the data outside the bump region are treated as a "regular" background as indicated by the solid line in Fig. 10.

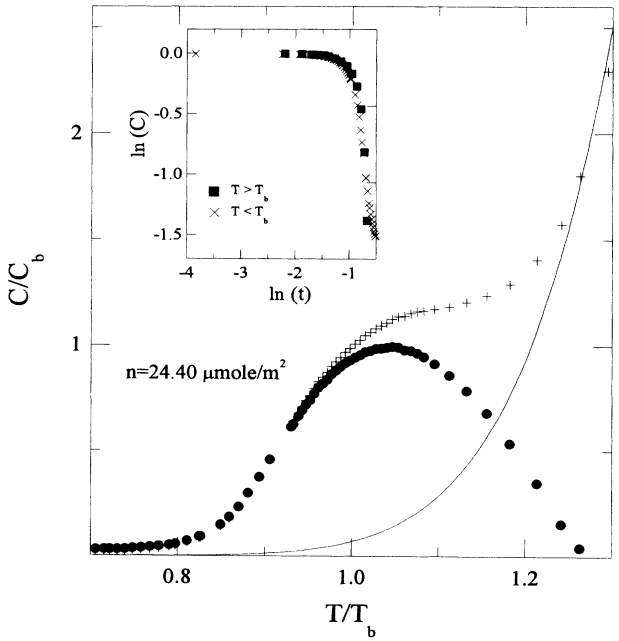

FIG. 10. Specific heat (+) as a function of temperature (after normalization by C_b and T_b) for a film in Anopore. The solid symbols represent the specific heat after subtraction of a "regular" background shown by the solid line obtained by fitting data outside the bump region. Inset: ln-ln plot after background subtraction.

When this background is subtracted from the specific heat results (normalized by C_b and T_b), a broad and extremely round peak is obtained. Such a peak is strongly dependent on the choice of background and given the extreme rounding, any attempt of critical behavior type of analysis is meaningless. A ln-ln plot of this specific heat data as a function of reduced temperature is shown in the inset to Fig. 10, where the sharp rise (with a slope of 3) is strongly a function of the chosen background. Thus, the bump is not a consequence of a phase transition.

Note that if heat-capacity isotherms were constructed from the temperature scans (see Ref. 31), for coverages up to 30 μmole/m^2 (some of which are superfluid at the lowest temperatures since $n_c \sim 20$ μmole/m^2), the heat capacity continuously increases. This is contrary to observations in porous glasses and in Nuclepore where the heat capacity decreased once the films became superfluid. This effect will be discussed further in a subsequent paper dealing with multilayer films.

B. Millipore

To investigate the role of disorder it would be desirable to have the ability to change the amount of disorder within a given experimental cell. Alternatively, but not totally equivalent, a similar effect may be achieved by using a different disordering substrate. Thus, after completing the Anopore runs, we turned to the Millipore cell that had been simultaneously cooled down. In spite of the multiple connection of its pores, the relevant length scales in Mullipore are such that helium films behave 2D-like.[20] Again, our heat-capacity measurements focus on coverages that are nonsuperfluid as established by comparison with the superfluid density measurements at Cornell[20] which determined the critical coverage for superfluid onset at $T=0$ K to be 24.6 μmole/m^2. As detailed below, the heat-capacity results in Millipore are remarkably similar to those in Anopore.

As in Anopore and with increasing coverage, the helium contribution becomes more important and deviates from the empty cell at progressively lower temperatures. In striking resemblance to the previous results, a heat-capacity bump centered at a temperature that decreases with coverage is found. Since the Millipore data are limited below 1 K, no information about a possible high-temperature anomaly is presently available. The low-temperature bump in Millipore also disappears once the coverage is such that the film is superfluid at the temperature where it would be expected. Specific heat results for films in Millipore after the empty cell subtraction are shown in Fig. 11. When the same data are normalized by the specific heat and temperature values at the middle of the bump, all films nicely collapse onto a universal curve shown in the inset to Fig. 11.

The Millipore bump is shape-wise more "flat" than the Anopore one, i.e., after the initial sharp rise above the background, the heat capacity does not increase as rapidly with temperature. This bump narrows from 250 to 170 mK with coverage, while the area remains constant at 2.7 mJ/mole, 30% less than in Anopore. As previously discussed, although the bump is a universal feature for dis-

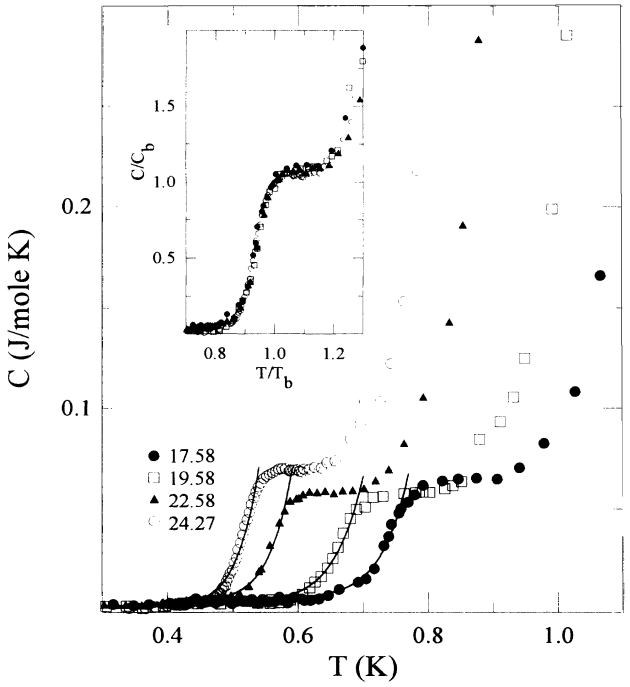

FIG. 11. Specific heat as a function of temperature for helium films in Millipore after empty cell subtraction. Solid lines represent fits according to Eq. (2). Inset: same data normalized by C_b and T_b. Coverages in μmole/m^2.

ordering substrates, the area are width probably quantify the interplay between disorder and Van der Waals attraction. The coverage dependence of the Millipore bump temperature position, Fig. 9, is not unlike that in Anopore; both behave differently from the nearly linear coverage dependence for the temperature break in Vycor which is also shown in Fig. 9. In Xerogel, there is curvature as in our substrates, but the bump can be followed to lower temperatures.

The Millipore results were also analyzed according to Eq. (2). This allows us to establish whether the previously obtained values for Δ are unique to Anopore or they are a reflection of the effect of the type of underlying substrate. From the fits to the data which are indicated by the solid lines in Fig. 11, we find that Δ/k_B decreases from 15.5 to 9 K for the films shown. Both the energy-gap magnitude and the bump temperature coverage dependence are similar to those in Anopore. Thus, a Δ/k_B an order of magnitude larger than in porous glasses appears to be typical of substrates where two-dimensional superfluid behavior is eventually exhibited. As in Anopore, and clearly seen from Fig. 9, a bump is seen for films that are superfluid at temperatures below the bump.

C. Mylar

It has been well established by many authors that the behavior of superfluid helium films in Mylar is well described by the two-dimensional Kosterlitz-Thouless theory.[32] It is thus natural to extend our localized layer studies to a planar substrate like Mylar. Aside from again offering a different "amount" of disorder that allows testing for the claimed universality of the observed features, a pore size distribution certainly present in Anopore or Millipore, would not play a role. We are convinced that a distribution of pore sizes is not having a significant effect in these results as the thickness of the films studied (and the reproducibility of the data under a variety of different conditions) is far from capillary condensation influence. If the bump were related to a pore size distribution, it would be expected to be more prominent in Millipore, contrary to our observations (see below). Even though the Mylar work is ongoing, it is important to report it here as it corroborates the previous results.

In spite of the lower surface area of the Mylar cell, our technique is sensitive enough that the helium signal is extracted with no more difficulty than for the other substrates. The resolution is aided by the large specific heat of these films. Specific heat results for a few films in Mylar are shown in Fig. 12 after empty cell subtraction. Once more, the disorder induced bump moving to lower temperatures with coverage is found. The area under the bump remains constant at 9 mJ/mole (a factor of 2 more than in Anopore) while narrowing from 220 mK for a 23.37 μmole/m^2, to 170 mK for the 30.48 μmole/m^2 film. The thick-film Mylar bump appears at the lowest temperature (0.48 K) than with either Anopore or Millipore. Interestingly, of the three substrates, Mylar is the one with largest critical coverage, 28 μmole/m^2.[21] The Mylar bump temperature position dependence on coverage is similar to that for the previous substrates but extends to lower temperatures as shown in Fig. 9. The 30.48 μmole/m^2 film is superfluid with a transition temperature at $\sim$0.16 K,[21] well below the bump temperature. Again, this supports the idea that the bump is a property of the normal component of the film.

For completeness, the Mylar data were fitted according

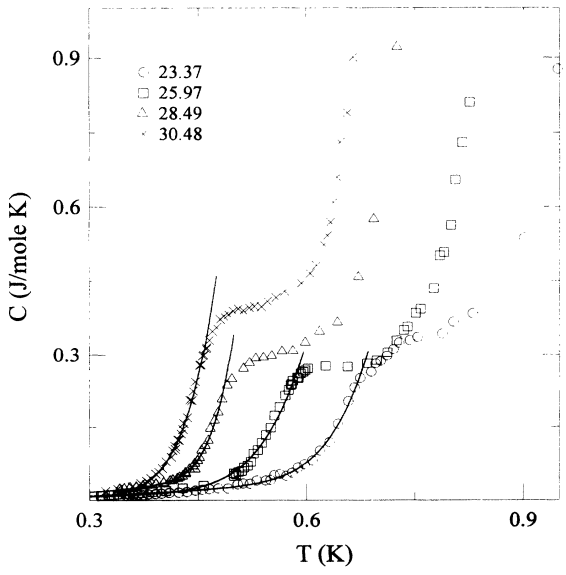

FIG. 12. Specific heat as a function of temperature for helium films in Mylar after empty cell subtraction. Solid lines represent fits to Eq. (2).

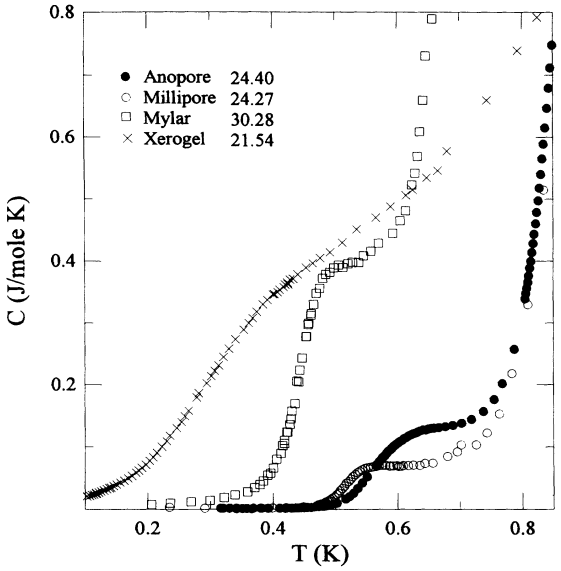

FIG. 13. Comparison of the specific heat bumps found in the three substrates. For each substrate, the film shown is that which exhibits the bump at the lowest temperature. Also included is a film in Xerogel from Ref. 9. Coverages in μmole/m^2.

to Eq. (2). From these fits, which are shown by the solid lines in Fig. 12, the magnitude of Δ is comparable to that of the previous substrates; it is 9.5 K for the highest temperature bump decreasing to $\Delta/k_B \sim 6$ K for the thickest film shown. This smaller value is a direct consequence of the lower temperature at which the bump is found for the Mylar substrate.

The results for each substrate are summarized and compared in Fig. 13. Here, we plot the specific heat for the film that shows the lowest temperature bump for each substrate. A major feature is that the specific heat in Mylar is considerably larger than in Anopore and Millipore which accounts for the bump's overall larger area despite being the narrowest. Such differences in specific heat also indicate that the film's excitation spectrum is strongly influence by the underlying substrate. Shapewise, the broader Anopore bump appears more rounded. The heat-capacity rise is steeper in Mylar than in Millipore and in Anopore. The specific heat for a film in Xerogel that shows a similar broad bump and with a low-temperature specific heat magnitude which is larger than for any of the substrates studied here, is also shown in Fig. 13 for comparison.

IV. SUMMARY AND CONCLUSIONS

We have presented a systematic heat-capacity study for localized helium films as a function of temperature, thickness, and disordering substrate as provided by Anopore membranes, Millipore fibrous filter paper, and Mylar polyester film. Even though the topology of the underlying substrate varies from cylindrical to interconnected to planar, nonsuperfluid helium films in these substrates behave in a remarkably similar fashion. A distinct heat-capacity bump whose position in temperature decreases with coverage is present for all substrates. The bump is viewed as a universal feature of helium films adsorbed in disorder-inducing substrates. The magnitude of the parameters that characterize it, namely, the area under the bump, its width and lowest temperature position are nonuniversal or substrate dependent. These are probably a measure of the "amount" of disorder introduced by the substrate and its interplay with the Van der Waals force.

Data were analyzed, using a model applicable to heterogeneous substrates where the localization of helium atoms is not strong enough, in such a way that long-range variations in the adsorbing potential give rise to large lateral pressures that are sufficiently strong to force helium atoms into patches or islands. Aspects of the data, like the sharp decrease in heat capacity with reducing temperature, are fitted reasonably well by such a model. The parameter Δ, which represents the barrier that needs to be overcome in order to promote the least strongly bound atoms out of an island and into a free particle or extended state, is found to have the same order of magnitude for all substrates used here while being a factor of 5 larger than in porous glasses. The magnitude of Δ decreases with increasing coverage and in fact is strongly related to the bump temperature position. If a particular set of data is simply shifted to lower temperature such that the bump is centered at temperatures in the vicinity of 0.2 K, the data are fitted equally well. But now with $\Delta/k_B \sim 1$ K, a magnitude which is comparable to that in the case of porous glasses where heat-capacity features were seen at lower temperatures, it is tempting to conclude that a larger Δ reflects a lower amount of disorder. A similar conclusion may be reached from a comparison of specific heats which are larger in porous glasses than in these substrates where films are intrinsically more ordered. In all cases, and as expected given the presumably richer excitation spectrum, the film's specific heat is larger than that of bulk helium.

Data analysis is suggestive that the density of states for the "localized" films is such that it includes excitations with an energy gap but not necessarily related to the idea of islands-type film growth. When the islands merge and superfluid behavior sets in, i.e., at the critical coverage, the gap energy should vanish. Although the magnitude of Δ and its coverage dependence are consistent with such a picture, Δ is not seen to continuously decrease towards zero; its lowest measured value is about 6 K. Further, as seen from Fig. 9, some of the films studied are superfluid and exhibit the heat-capacity bump at temperatures above the superfluid transition. Thus, the heat-capacity data are suggestive of the presence of "gap" excitations, yet, such a gap does not arise from an "island" type of film formation. Even though our understanding of the localized layer is incomplete, it is nonetheless clear that it is not inert.

The specific heat bump disappears once the coverage is such that the films' superfluid behavior should be manifest at the temperature where the bump would be expected, in agreement with observations in porous glasses. The lowest temperature at which the bump is seen is about 0.5 K, being lowest for the substrate with the largest critical coverage, i.e., Mylar. Xerogel porous glass

nicely fits in this picture since its critical coverage is at 32 μmole/m^2 and shows a bump at temperatures as low as 0.235 K. Thus, the stronger the Van der Waals attraction to the substrate, the lower the temperature at which the bump would be found. The critical coverages for each substrate are indicated by the symbols on the coverage axis of Fig. 9. The Vycor results do not fit into this picture. Again, there appears to be a uniqueness in the behavior of helium in Vycor.

Theoretical predictions for the specific heat treating the influence of substrate disorder and including the real presence of the Van der Waals interactions are desirable. In addition, several experiments can be performed that would equally contribute and provide a more complete framework for theoretical studies. The addendum heat capacity needs to be decreased by at least an order of magnitude to reliably extract the heat-capacity temperature dependence. This is extremely important in order to compare with existing theoretical predictions, in particular, the linear specific heat typical of disordered systems. Such a minimization would be difficult to achieve for a Mylar cell as it would carry a simultaneously large loss of the already small surface area. In Anopore or Millipore, one could conceivably design an open cell and probe a single membrane or filter provided with thermometer and heater. The obvious drawback of this scenario is that again, due to the low surface area, evaporation effects could play a dominant role.

Despite the unfortunately large background of our cells, it would still be extremely informative to preplate the substrate with, for instance, one or two layers of nitrogen or hydrogen. Since it is well known that preplating would smooth out the substrate and decrease the Van der Waals attraction, one would be able to determine how important a role the detailed form of the underlying potential plays, or if the only effect is that of shifting the helium coverage scale.[7] One might then be able to better characterize the interplay between disorder and the Van der Waals attraction. Although the latter appears to be unimportant for the critical behavior, it is clearly of relevance for localized films. As discussed in Ref. 3, in the absence of disorder and at $T=0$ K, the Van der Waals attraction stabilizes a self-bound superfluid liquid phase in coexistence with a zero density vapor. If the disorder is large compared to the attractive interaction, the phase separation is destroyed and the transition to superfluidity is likely to be continuous.

In summary, there is a fair amount of knowledge that can be extracted from studies of localized helium films. Our work is another step in that direction that will hopefully stimulate further experimental and theoretical work. Anopore membranes are a particularly suitable substrate that will be extensively used to study a variety of systems and phenomena. Our recent studies of phase transition for liquid crystals confined to these membranes are a good example.[33]

ACKNOWLEDGMENTS

We are indebted to John Reppy for providing us with Refs. 8 and 20, to Oscar Vilches for Ref. 29, and to Mirko Gnan for his help in the construction of the Mylar cell. This work was supported by NSF Low Temperature Physics Program Grant No. DMR 90-13979.

*Present address: Department of Physics, Penn State University, University Park, PA 16802.

[1]J. A. Hertz, L. Fleishman, and P. W. Anderson, Phys. Rev. Lett. **43**, 942 (1979).

[2]M. Ma, B. I. Halperin, and P. A. Lee, Phys. Rev. B **34**, 3136 (1986).

[3]M. P. A. Fisher, P. B. Weichman, G. Grinstein, and D. S. Fisher, Phys. Rev. B **40**, 546 (1989).

[4]W. Krauth, N. Trivedi, and D. Ceperley, Phys. Rev. Lett. **67**, 2307 (1991).

[5]D. K. K. Lee and J. M. F. Gunn, J. Phys. Condens. Matter **2**, 7753 (1990); **4**, 1729 (1992).

[6]D. F. Brewer, J. Low Temp. Phys. **3**, 205 (1970); D. F. Brewer, A. Evenson, and A. L. Thomson, *ibid.* **3**, 603 (1970).

[7]R. H. Tait and J. D. Reppy, Phys. Rev. B **20**, 997 (1979).

[8]F. W. Van Keuls, P. A. Crowell, and J. D. Reppy (unpublished); P. A. Crowell, Ph.D. thesis, Cornell University, 1994 (unpublished).

[9]D. Finotello, A. Wong, K. A. Gillis, D. D. Awschalom, and M. H. W. Chan, Jpn. J. of Appl. Phys. **26**, Supp. 3, 283 (1987).

[10]D. Finotello, K. A. Gillis, A. Wong, and M. H. W. Chan, Phys. Rev. Lett. **61**, 1954 (1988).

[11]B. K. Bhattacharyya, M. J. DiPirro, and F. M. Gasparini, Phys. Rev. B **30**, 5029 (1984).

[12]W. F. Saam and M. W. Cole, Phys. Rev. B **11**, 1086 (1975).

[13]Anopore available from Whatman Laboratory Div., 9 Bridewell Place, Clifton, NJ 07014.

[14]Millipore Corporation, 80 Ashby Rd., Bedford, MA 01730.

[15]Mylar, a trademark of the duPont Company.

[16]R. C. Furneaux, W. R. Rigby, and A. P. Davidson, Nature **337**, 147 (1989).

[17]T. P. Chen, M. J. DiPirro, B. K. Bhattacharyya, and F. M. Gasparini, Rev. Sci. Instrum. **51**, 846 (1980); T. P. Chen, M. J. DiPirro, A. A. Gaeta, and F. M. Gasparini, J. Low Temp. Phys. **26**, 927 (1977).

[18]P. Levitz, G. Ehret, S. K. Sinha, and J. M. Drake, J. Chem. Phys. **95**, 8 (1991).

[19]G. P. Crawford, L. M. Steele, R. Ondris-Crawford, G. S. Iannacchione, C. J. Yeager, J. W. Doane, and D. Finotello, J. Chem. Phys. **96**, 7788 (1992).

[20]D. F. McQueeney, Ph.D. thesis, Cornell University, 1988 (unpublished).

[21]G. Agnolet, D. F. McQueeney, and J. D. Reppy, Phys. Rev. B **39**, 8934 (1989).

[22]P. F. Sullivan and G. Seidel, Phys. Rev. **173**, 679 (1968).

[23]L. M. Steele, G. S. Iannacchione, and D. Finotello, Rev. Mex. Fis. **39**, 588 (1993).

[24]L. M. Steele, C. J. Yeager, and D. Finotello, Phys. Rev. Lett. **71**, 3673 (1993).

[25]J. G. Dash, J. Low Temp. Phys. **1**, 173 (1969); G. A. Stewart and J. G. Dash, Phys. Rev. A **2**, 918 (1970).

[26]C. J. Yeager, L. M. Steele, and D. Finotello (unpublished).

[27]S. W. Van Sciver and O. E. Vilches, Phys. Rev. B **18**, 285 (1978).

[28]N. N. Roy and G. D. Halsey, J. Low Temp. Phys. **4**, 231 (1971).
[29]J. G. Daunt, Phys. Lett. **41A**, 223 (1972).
[30]S. W. Van Sciver, Ph.D. thesis, University of Washington, 1976 (unpublished).
[31]L. M. Steele and D. Finotello (unpublished).
[32]J. Maps and R. B. Hallock, Phys. Rev. Lett. **47**, 1533 (1981); G. Agnolet, S. L. Teitel, and J. D. Reppy, *ibid.* **47**, 1537 (1981); D. Finotello and F. M. Gasparini, *ibid.* **55**, 2156 (1985); D. Finotello, Y. Y. Yu, and F. M. Gasparini, Phys. Rev. B **41**, 10 994 (1990).
[33]G. S. Iannacchione and D. Finotello, Phys. Rev. Lett. **69**, 2094 (1992).

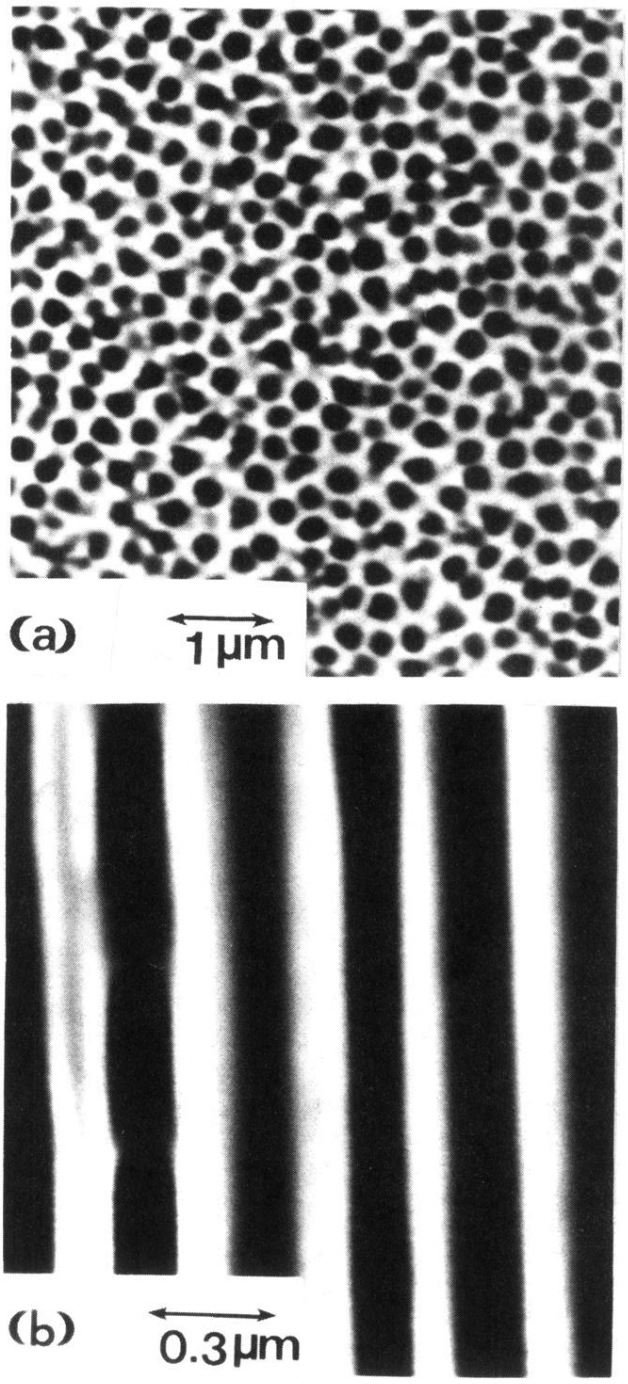

FIG. 1. Scanning electron microscopy photographs for an Anopore membrane. (a) top view (b) cross sectional view.

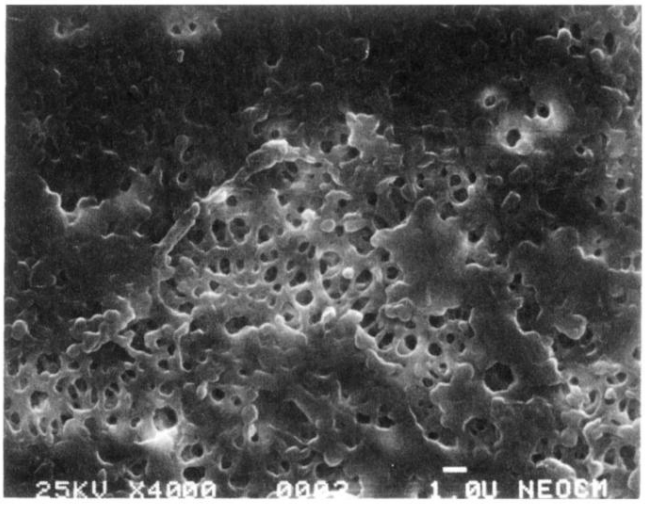

FIG. 3. Scanning electron microscope photograph for a Millipore filter paper.